Nonlocal screening effects on core-level photoemission spectra investigated by large-cluster models

Kozo Okada*
Faculty of Education, Yamaguchi University, 1677-1, Yoshida, Yamaguchi 753, Japan

Akio Kotani†
Institute for Solid State Physics, University of Tokyo, 7-22-1, Roppongi, Minato-ku, Tokyo 106, Japan
(Received 3 March 1995)

The copper $2p$ core-level x-ray photoemission spectrum in CuO_2 plane systems is calculated by means of large-cluster models to investigate in detail the nonlocal screening effects, which were pointed out by van Veenendaal *et al.* [Phys. Rev. B **47**, 11 462 (1993)]. Calculating the hole distributions for the initial and final states of photoemission, we show that the atomic coordination in a cluster strongly affects accessible final states. Accordingly, we point out that the interpretation for Cu_3O_{10} given by van Veenendaal *et al.* is not always general. Moreover, it is shown that the spectrum can be remarkably affected by whether or not the O $2p_\pi$ orbits are taken into account in the calculations. We also introduce a Hartree-Fock approximation in order to treat much larger-cluster models.

I. INTRODUCTION

Recently, nonlocal screening effects on core-level x-ray photoemission spectra (XPS) have been discussed for oxide superconductors and NiO by van Veenendaal and coworkers by means of exact diagonalization calculations.[1–4] According to their result on the Cu_3O_{10} cluster,[2] charge transfer from the neighboring CuO_4 units as well as from the nearest O $2p$ orbits takes place in order to screen the core-hole charge in the photoemission final state. Moreover, the final state reached by the former process is lower in energy than that by the latter one, and consequently the former one contributes more to the main peak in the XPS. Thus their interpretation for the Cu $2p$ XPS is considerably different from the analysis based on the single Cu site model, such as a CuO_4 cluster model or an Anderson impurity model.[5–9]

However, it is not trivial why the multiple Cu site model and the standard single-site Anderson impurity model appear to give considerably different results. There is a general consensus that a hole doped in CuO_2 plane systems moves mainly on the O $2p$ orbits, forming a Zhang-Rice singlet.[10] If so, we can expect that the hole which is pushed out from the core-hole site owing to the core-hole potential in the photoemission final state would also move mainly on the O $2p$ orbits. In the present study, we calculate the hole distributions for the ground and final states of the core-level photoemission for various cluster models to discuss the nonlocal screening effects in detail.

It is evident that the multiple Cu site effects pointed out by van Veenendaal and co-workers cast a new light on the excited-state structure of strongly correlated systems. On the other hand, it seems that correspondence of the calculated spectrum to the experimental one is not perfect, since the main peak in the former consists of only two intense lines separated by about 2 eV, which could be resolved experimentally. This point was not improved even in the calculated result for the Cu_5O_{16} cluster.[4] As for this, we shall point out that the convergence of the spectral shape could not be attained for such small clusters by exact diagonalization calculations, and that the O $2p_\pi$ orbits should also be taken into account. On the other hand, it is very difficult to extend the cluster size because the size of the Hamiltonian matrix increases too rapidly. In this paper, therefore, we introduce a Hartree-Fock (HF) approximation for the electron correlation on Cu sites away from the core-hole site in order to take into account the multiple Cu site effects. Using the obtained HF orbits, we make standard configuration-interaction (CI) calculations.[5–9] This approximation can greatly reduce the size of the Hamiltonian matrix to be solved.

The rest of the present paper is organized as follows: In Sec. II, we describe the model Hamiltonian. In Sec. III, we show the Cu $2p$ XPS calculated for various clusters consisting of several Cu sites, together with the hole distributions in the ground state and the final states of photoemission. They were obtained by exact diagonalization calculations. In Sec. IV, we introduce a Hartree-Fock approximation in order to treat larger clusters. Based on these results, we discuss the multiple Cu site effects in Sec. V, comparing with the results by a single Cu site model. In some calculations, we take into account the apical oxygens and the Cu $3d_{3z^2-r^2}$ orbits. In Sec. VI, we summarize the results obtained in the present paper.

II. CLUSTER MODEL

We start with the d-p model, the Hamiltonian of which is given in hole picture by

$$H_0=\sum_{i,s}\varepsilon_d n_{dis}+\sum_{j,s}\varepsilon_p n_{pjs}+\sum_{\langle i,j\rangle,s}V_{pd}(d_{is}^{\dagger}p_{js}+p_{js}^{\dagger}d_{is})+\sum_{\langle j,j'\rangle,s}V_{pp}(p_{js}^{\dagger}p_{j's}+p_{j's}^{\dagger}d_{js})+U_{dd}\sum_i n_{di\uparrow}n_{di\downarrow}\,, \tag{1}$$

 ©1995 The American Physical Society

where $d_{is}^{\dagger}(p_{js}^{\dagger})$ creates a hole with spin s on the ith Cu $3d_{x^2-y^2}$ orbit (the jth O $2p_{\sigma}$ orbit). In some cases shown later, we also take into account the Cu $3d_{3z^2-r^2}$ and O $2p_{\pi}$ orbits. The first and second terms on the right-hand side of Eq. (1) represent the one-body energies, where $n_{dis}(n_{pjs})$ is the number operator for the Cu $3d$ (O $2p$) hole. We define the charge-transfer (CT) energy as $\Delta \equiv \varepsilon_p - \varepsilon_d$. The third term represents the hybridization of the Cu $3d$ and O $2p$ orbits, where $\langle i,j \rangle$ denotes the summation over the nearest-neighbor pairs. The fourth and last terms represent the hybridization of the neighboring O $2p$ orbits and the Coulomb repulsion between the $3d$ holes, respectively. In the final state of the Cu $2p$ XPS, the core hole created at site 0 interacts with the $3d$ holes. The interaction Hamiltonian is given by

$$H_c = U_{dc} \sum_s n_{d0s} n_c \ , \tag{2}$$

where n_c is the number operator for the core hole. For simplicity, we disregard the multiplet coupling effects. The numerical values for Δ (=3.5 eV), U_{dd}(=8.8 eV), U_{dc}(=7.7 eV), $pd\sigma$(=1.5 eV), $pp\sigma$(=−1.0 eV), and $pp\pi$(=0.3 eV) are the same as those used by van Veenendaal and co-workers.[2–4]

The Cu $2p$ XPS is calculated by

$$I(E_B) = \mathrm{Im}\langle g | \frac{1}{E_B - (H_0 + H_c) + E_g} | g \rangle \ , \tag{3}$$

where $|g\rangle$ is the wave function for the ground state, which is obtained by diagonalizing H_0. The continuous spectrum is obtained by convoluting with a Gaussian function of width 0.2, 1.5, or 2.0 eV.

III. EXACT CALCULATIONS

A. Cu_3O_{10}

In Fig. 1(a), the experimental spectrum[2] is shown with a dotted curve. In consists of a main structure (1–5 eV) and the satellite (9–13 eV). The rectangular line shape of the satellite is due to the multiplet coupling of the Cu $3d$ and $2p$ holes.[7,11] However, the multiplet effect is disregarded in the present study for simplicity, since it hardly affects the line shape of the main structure, the intensity ratio of the satellite to the main structure and the energy separation of the main structure and the satellite. However, we note that the convolution width of about 2 eV for theoretical spectra shown below is too large from the multiplet structure calculation so far made for the satellite.

The following results were obtained by the recursion method.[12] First of all, we reproduce the Cu $2p$ XPS for Cu_3O_{10} with three holes in Fig. 1(a), where the atomic coordination used is also depicted. A core hole is created on the central Cu site. Figure 1 is the same as that given by van Veenendaal, Eskes, and Sawatzky,[2] except that the linewidth used is smaller than theirs (=2.0 eV). We consider that, with the width of 1.5 eV, the main peak ap-

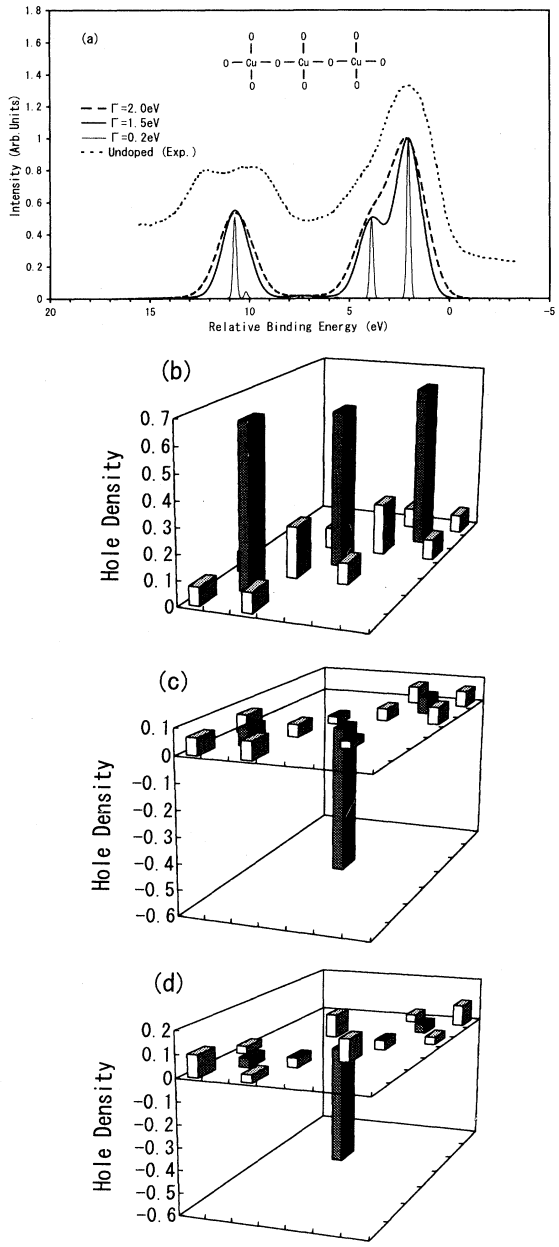

FIG. 1. (a) shows the Cu $2p$ XPS for Cu_3O_{10} with three holes (one up-spin and two down-spins) obtained by exact diagonalization. For each spectrum, the maximum of the leading peak is normalized to unity. The experimental Cu $2p_{3/2}$ XPS taken from Ref. 2 is also plotted for comparison. The rectangular shape of the satellite is due to the $2p^5 3d^9$ multiplet splittings, which is not taken into account in the present calculation. (b) shows the hole distribution in the ground state. The basal plane corresponds to the atomic coordination shown in the inset of (a). Dark and bright boxes on the basal plane represent hole densities at the atomic sites of Cu_3C_{10}. The former and latter correspond to Cu and O sites, respectively. In (c) and (d), the deviation of hole distribution from the ground state is calculated for the lowest and next-lowest final states, respectively. Boxes having a black surface on top represent that the hole density is decreased on those atoms in the photoemission final state.

parently splits, which is inconsistent with the experimental result. The intensity ratio of the satellite to the main structure is 0.34, and the peak separation is about 8.5 eV.

In Fig. 1(b), we show the hole distribution in the ground state, which was also given by van Veenendaal, Eskes, and Sawatzky. In Fig. 1(b), we find that the hole densities in the Cu sites are approximately the same, while those in the O $2p$ sites differ considerably for the O $2p$ orbits which connect two Cu $3d$ orbits and those which couple only to one $3d$ orbit. This difference is evidently a kind of *surface effect*. Figure 1(c) shows the deviation of the hole distribution from the ground state for the lowest-energy final state. Figure 1(d) is that for the next-lowest final state. The hole pushed out from the core-hole sites moves to the neighboring CuO_4 units in Fig. 1(c), as pointed out by van Veenendaal, Eskes, and Sawatzky. In Fig. 1(d), on the other hand, the hole moves to the edges of the cluster. This point can be understood more clearly, comparing with the results for Cu_5O_{16} shown below.

B. Square planar Cu_5O_{16}

In Fig. 2(a), we show the calculated Cu $2p$ XPS for a square planar Cu_5O_{16} cluster. This cluster was already used by Nishino[13] and van Veenendaal and Sawatzky.[4] A core hole is created on the central Cu site. The main structure consists of two intense lines, as in the case of Cu_3O_{10}. The calculated intensity ratio is 0.31. However, the energy separation of two lines consisting of the main structure is larger in Cu_5O_{16} than in Cu_3O_{10}. As a result, the main structure splits even in the case of width 2.0 eV.

Since Nishino and van Veenendaal and co-workers did not discuss the details of the final states, we compare the hole distributions with those for Cu_3O_{10}. The hole distribution in the ground state is shown in Fig. 2(b), and the deviation from the ground state is shown in Figs. 2(c) and 2(d) for the two final states consisting of the main structure, respectively. In Fig. 2(c), which is for the lowest final states, we find that the hole pushed out from the core-hole site moves to the neighboring CuO_4 units, as in the case of Cu_3O_{10}. It is sure that the hole moves mainly on the O sites, since the weight is 75% on the O sites and 25% on the Cu sites. On the other hand, we find in Fig. 2(d), which is for the next lowest state, that the hole pushed out moves mainly to four corners of the cluster. The weight on the nearest-neighbor O sites is only 9%. This hole distribution is quite different from Fig. 1(d), irrespective of the fact that the spectral weight and the binding energy do not differ so much for these two cases. When we compare the average radius of the screening cloud in Fig. 2(c) with that in Fig. 2(d), the former is obviously smaller than the latter. In other words, the screening cloud extends more in the final states having higher energies. This is a contrast to the case of Cu_3O_{10}. Therefore we understand that atomic coordination strongly affects accessible final states. We consider that the final state giving the second line at 4 eV in Fig. 1(a) differs considerably from that in Fig. 2(a). The resemblances between them seem to be accidental.

C. Chainlike Cu_5O_{16}

To check the convergence of the spectral shape with respect to the cluster size, we show the result for a chainlike Cu_5O_{16} cluster with five holes (two down- and three up-spins) in Fig. 3(a). It appears that the second line at 4 eV in Cu_3O_{10} splits into three lines in Cu_5O_{16}. Therefore we conclude that the double-line feature of the main

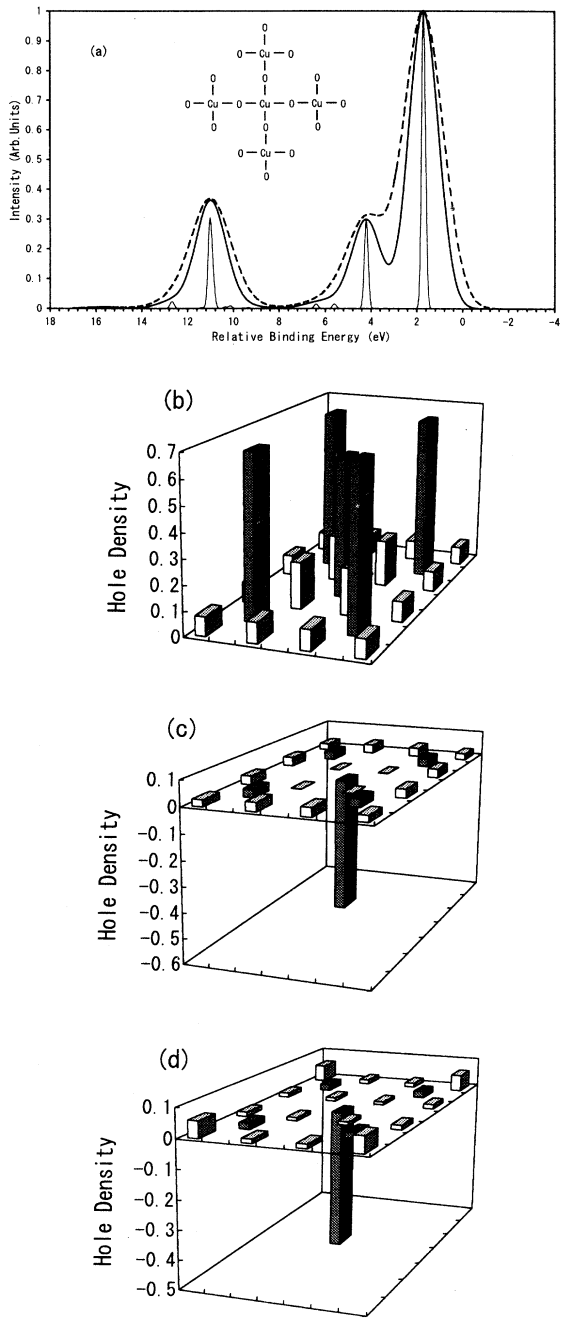

FIG. 2. (a) shows the Cu $2p$ XPS for square planar Cu_5O_{16} with five holes (one up-spin and four down-spins) obtained by exact diagonalization. For (b), (c), and (d), see the caption for Figs. 1(b)–1(d).

structure in Cu_3O_{10} is not always valid for large clusters. When we compare the continuous spectrum with a width of 1.5 eV, the line shape of the main structure differs from that in Cu_3O_{10} or the square planar Cu_5O_{16}. In this sense, the convergence of the spectral shape is not attained with Cu_3O_{10} or probably even with Cu_5O_{16}. The intensity ratio of the satellite to the main structure is also about 0.39, which is somewhat larger than that in Cu_3O_{10} (=0.34).

The hole distribution in the ground state is shown in Fig. 3(b). The deviation of the hole density from the ground state is shown for the lowest final state in Fig. 3(c). In Fig. 3(c), we find that the screening cloud is fairly extended in space. The maximum hole density is observed in the O 2*p* orbits connecting two Cu sites. It seems to reflect the motional effects of a Zhang-Rice singlet state. This is in contrast to the case of Cu_3O_{10}, where the Zhang-Rice singlet can no longer move anymore because the cluster size is too small. As far as the excitation energy for the lowest state is concerned, however, the influence of the different hole distributions is fairly small, as can be seen in Figs. 1(a) and 3(a).

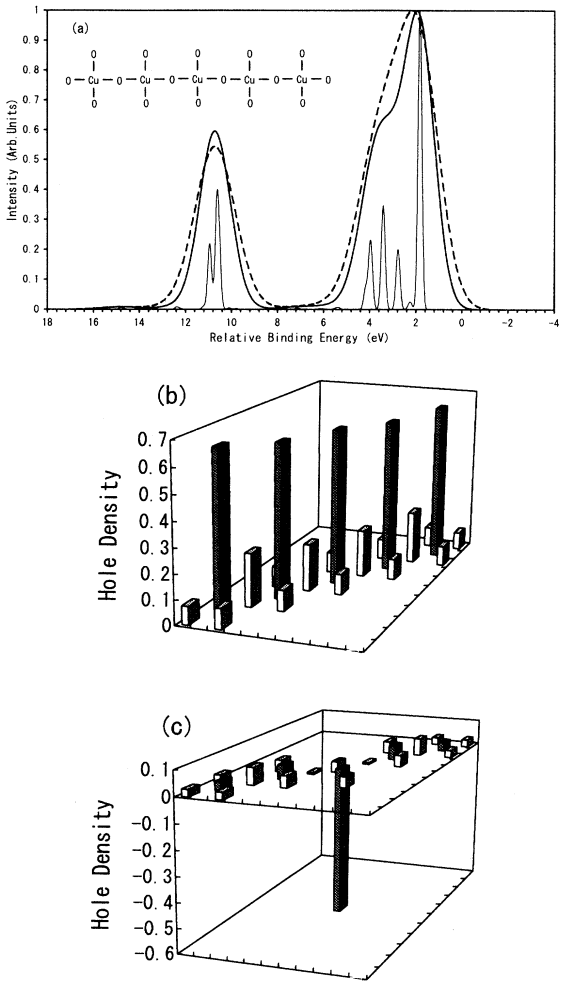

FIG. 3. (a) shows the Cu 2*p* XPS for chainlike Cu_5O_{16} with five holes (three up- and down-spins) obtained by exact diagonalization. For (b) and (c), see the caption for Figs. 1(b) and 1(c).

IV. HF-CI APPROXIMATION

A. Square planer Cu_5O_{16}

In order to treat larger clusters, we introduce a HF approximation for the hole correlation on Cu sites away from the core hole site. First of all, we divide the system into two parts: host and impurity systems. In principle, how to divide the system is arbitrary. We should take a better approach, judging from the convergence in spectral shape, for example. In the case of the square planar Cu_5O_{16} cluster discussed above, for example, the central Cu site and the others are mainly occupied by an up-spin and four down-spin holes, respectively, in the ground state. Let us take the central Cu ion as the impurity system. The other part of Cu_5O_{16} is treated as the host system. As for the holes, it seems reasonable to put one up-spin hole on the impurity system (central Cu) and the other down-spin holes on the host. For the host system, we perform a standard HF calculation to obtain molecular orbits (MO's). Combining the unoccupied MO's and the impurity system, we make a single-site Anderson model calculation to obtain the photoemission spectrum. We also use these MO's to calculate the photoemission final states.

A HF calculation for the host gives 20 unoccupied MO's for up-spin. The interaction strength of each MO to the impurity 3*d* orbit is determined by the wave-function amplitude and symmetry of the O 2*p* orbits surrounding the impurity. When we switch on the *p-d* hybridization between the impurity and the host, the up-spin hole on the impurity can move onto those MO's. Then the size of the effective Hamiltonian matrix is 21 (=20+1), which is much smaller than that for the exact calculation ($=_{21}C_1 \times {}_{21}C_4 = 125\,685$).

Using the obtained MO's, we make a standard CI calculation. According to the CI approach,[5–9,11] we call the state where the central Cu has one hole the $3d^9$ state. The states where the hole moves to the MO's corresponds to the $3d^{10}\underline{L}$ states, where $\underline{L}$ denotes a ligand hole. In the final state of photoemission, the energy of the $3d^9$ state is increased by U_{dc}. Therefore the main structure and the satellite of the Cu 2*p* XPS are due mainly to the $3d^{10}\underline{L}$ and $3d^9$ states, respectively. Actual wave functions for the ground and final states are described by linear combinations of $3d^9$ and $3d^{10}\underline{L}$ states. Since only a limited number of $3d^{10}\underline{L}$ states couple strongly to the $3d^9$ state, a small number of final states contribute to the main structure of the Cu 2*p* XPS. The calculated result for the Cu_5O_{16} cluster is shown in Fig. 4(a). We find that the result approximately reproduces the exact result shown in Fig. 2(a). The intensity ratio of the satellite to the main structure is 0.33, which coincides well with that in Fig. 2(a) (=0.31), although the intensity ratios between the peaks at about 2, 4, and 11 eV (thin solid curve) are somewhat different from those in Fig. 2(a). We can also show that the hole distribution for each final state which contributes to the spectrum is approximately the same as

that in the exact result. Thus the present approximation can greatly reduce lengthy calculations, giving reasonable results.

For comparison, we show the Cu $2p$ XPS for Cu_5O_{16} in Fig. 4(b), which was calculated also taking into account the O $2p_\pi$ orbits. As found from the curve of width 1.5 eV, the main structure shows a fairly smooth asymmetric shape, in contrast to Figs. 2(a) or 4(a). In the ground state, the hole occupation is less than 0.001 for the p_π orbits, while it is about 0.08 for the p_σ orbits. Accordingly one can disregard the $2p_\pi$ orbits in order to discuss only the ground-state properties. However, these orbits can be important in the photoemission final states. Thus it is important to take into account both the O $2p_\sigma$ and $2p_\pi$ orbits as well as the multiple Cu effects in order to reproduce the experimental line shape.

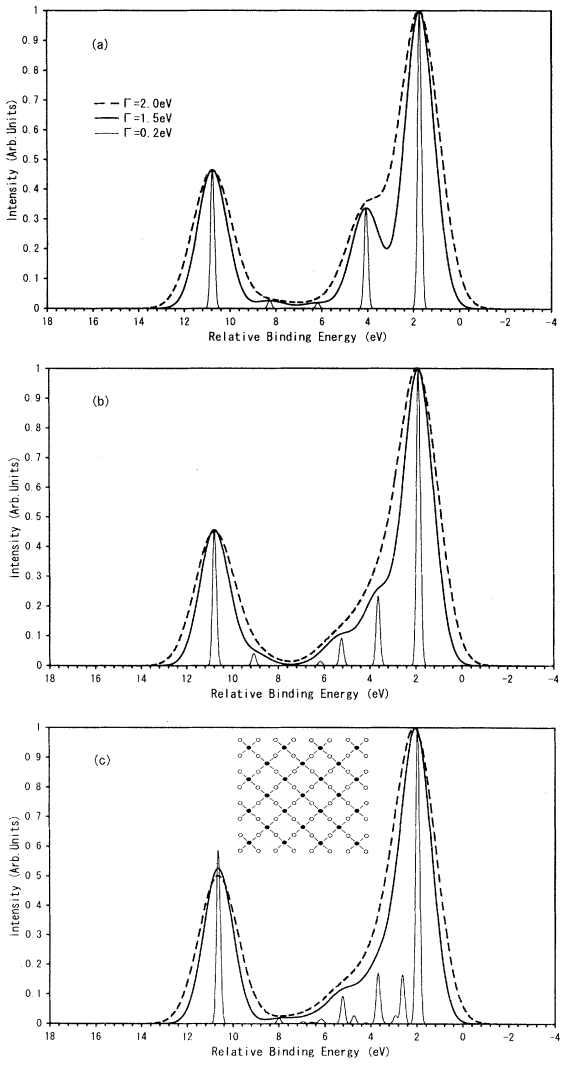

FIG. 4. (a) and (b) are the Cu $2p$ XPS's for Cu_5O_{16}. In the latter, the O $2p_\pi$ orbits are taken into account, while they are not in the former. Also in the Cu $2p$ XPS for $Cu_{25}O_{64}$ shown in (c), they are taken into account. These spectra are obtained by the present HF-CI calculation.

B. Square planar $Cu_{25}O_{64}$

Our HF-CI theory can be applied easily to larger clusters. As an example, we show the Cu $2p$ XPS for $Cu_{25}O_{64}$ in Fig. 4(c). In this case, the host is $Cu_{24}O_{64}$ with eight up-spin and 15 down-spin holes, and the impurity system is the central Cu having two holes (up- and down-spins). A HF calculation results in the antiferromagnetic ordering for the host. The average hole occupation in the Cu sites is about 0.6. As for the O sites, it is 0.07–0.1 for four O sites surrounding the central Cu site and for 12 edge sites. In the other O sites, it amounts to 0.15–0.2. Comparing Figs. 4(c) and 4(b), the convergence with respect to the cluster size is almost attained for width 1.5–2.0 eV, though it is not for the case of width 0.2 eV. The intensity ratio is 0.39, which is larger than that in Fig. 4(b) (=0.33). The intensity ratio thus increases slightly with the cluster size, as also seen in the exact results for chainlike Cu_3O_{10} and Cu_5O_{16} shown above.

V. DISCUSSIONS

In general, it is not easy to estimate the intensity ratio between the main structure and the satellite definitely, because of difficulties in subtracting the background contributions from the raw data uniquely. For example, we obtained 0.45–0.55 for $Bi_2Sr_2YCu_2O_{8.51}$ shown in Fig. 1, while van Veenendaal and co-workers value was 0.3–0.4. Therefore it is not easy to discuss the intensity ratio in detail. In our impression, however, the value of 0.3–0.4 seems somewhat too small. Accordingly, the theoretical values ranging 0.3 to 0.4 in the present calculations seem somewhat smaller than the experimental value, which is in clear contrast to the CuO_4 cluster model in which the intensity ratio may be somewhat too large with the present parameter values. We consider that this situation can be improved by introducing the electron configuration dependence of the *p-d* hybridization strength.[14,15] When the *p-d* hybridization is weakened owing to core-hole creation, the hybridization effects in the final state are so suppressed that the theoretical intensity of the satellite can be comparable with the experimental one. We can show that the reduction factor of 0.75 for the hybridization strength, which was calculated for CuO by Karlsson, Gunnarsson, and Jepsen,[15] actually improves the intensity ratio, as shown in Fig. 5. We thus consider that the multiple Cu site effects and the configuration-dependent hybridizations are necessary to discuss the intensity ratio in detail.

Let us discuss the roles of apical oxygens and Cu $3d_{3z^2-r^2}$ orbits as another factor to be taken into account in discussing the line shape. Although van Veenendaal, Eskes, and Sawatzky[2] concluded that the influence of Cu $3d_{3z^2-r^2}$ is small, we point out that this is not true when the system has the apical oxygens. In Fig. 6(a), we show the Cu $2p$ XPS for Cu_3O_{10}, in which the apical O $2p_\sigma$ orbits and Cu $3d_{3z^2-r^2}$ are also take into account. (The O $2p_\pi$ orbits are not taken into account.) The hybridization strengths used were scaled according to Harrison's text,[16] using the lattice constants for La_2CuO_4. We find that three lines appear around 4 eV in Fig. 6(a), in which re-

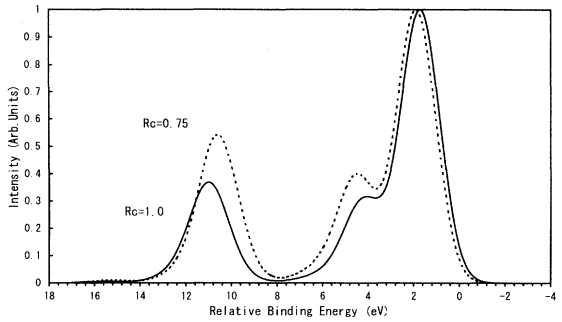

FIG. 5. The dotted spectrum is the Cu $2p$ XPS for Cu_5O_{16} calculated by taking into account the reduction effect of p-d hybridization. The reduction factor is 0.75. The solid spectrum is the same as the thick solid spectrum in Fig. 2(a).

gion there is only a single line in Fig. 1(a). The origin of the splitting is that, in the present model, the hole pushed out from the core-hole site can form a $(3z^2-r^2, x^2-y^2)$-type singlet or triplet as well as a Zhang-Rice singlet. Similar effects are seen in the Cu $2p$ XPS for Cu_5O_{16} shown in Fig. 6(b). Without the apical oxygens, however, the intensities for these final states are suppressed, as van Veenendaal and co-workers concluded.

In Fig. 7(a), we show Cu $2p$ XPS by means of CuO_{16} with one hole, where $2p_\pi$ orbits are not taken into account. The main peak consists of two components, as in the case of Cu_5O_{16} shown in Fig. 2(a). However, the line

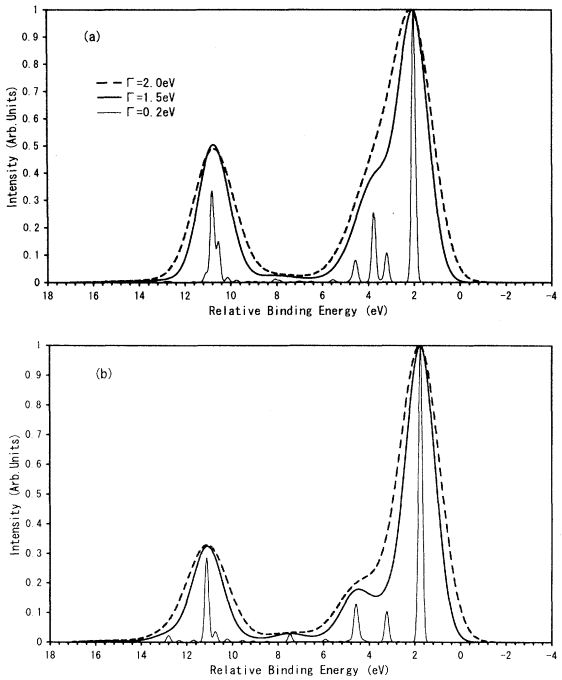

FIG. 6. (a) and (b) shows the Cu $2p$ XPS for Cu_3O_{10} and Cu_5O_{16}, where the $3d_{3z^2-r^2}$ and the apical oxygens are also taken into account. They are obtained by exact diagonalization calculations.

around 4 eV is fairly weaker than in Cu_5O_{16}. The intensity ratio of the satellite to the main structure is 0.44, which is somewhat larger than that in Figs. 2(a) or 4(a). The peak separation is about 8 eV, which is smaller than that in Figs. 2(a) or 4(a) by about 0.5 eV. We show the hole distribution for the ground state in Fig. 7(b), where we find that the hole is almost localized around the central CuO_4 unit. The deviations from the ground state are

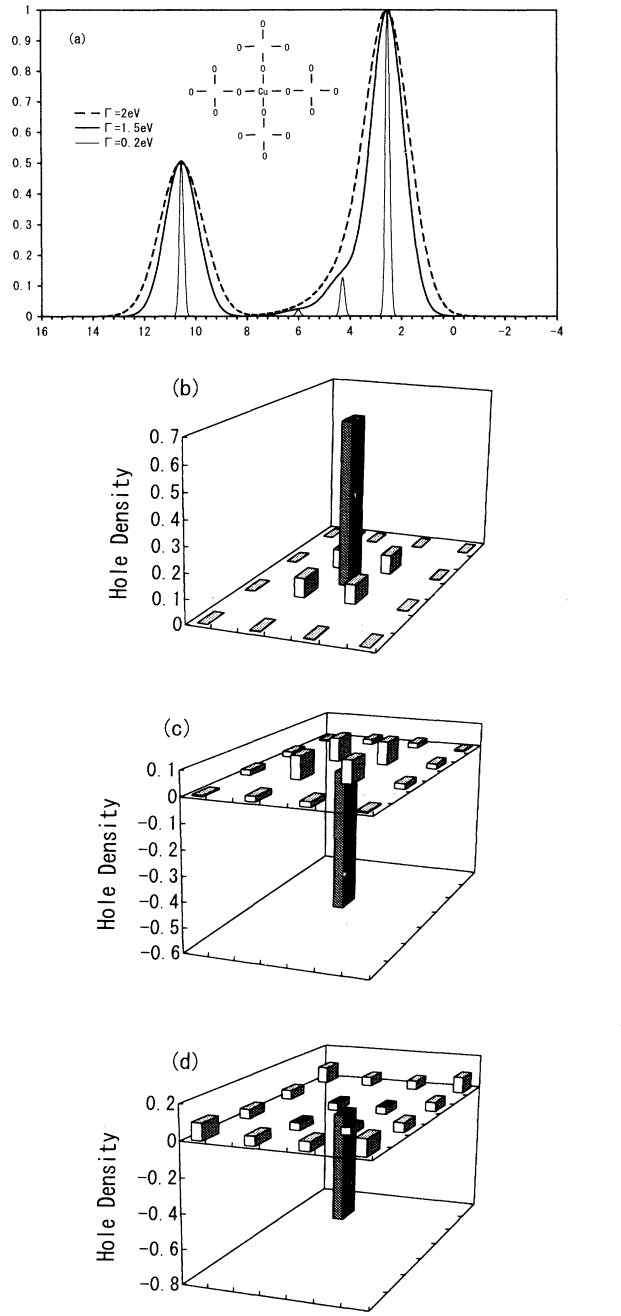

FIG. 7. (a) shows the Cu $2p$ XPS for CuO_{16} obtained by exact diagonalization. For (b), (c), and (d), see the caption for Figs. 1(b)–1(d).

shown for the lowest and next-lowest final states in Figs. 7(c) and 7(d), respectively. In Fig. 7(c), the hole pushed out moves to the nearest and next-nearest oxygen sites in the ratio 7:3, which is in a clear contrast to the case of Cu_5O_{16}, where the hole pushed out is mainly attracted around the next-nearest O sites. In Fig. 7(d), the hole pushed out moves to the edges of the cluster, as in the case of Cu_5O_{16}. In the present case, moreover, the hole densities at the nearest O sites are also decreased. Thus the hole redistribution takes place more radically in CuO_{16} than in Cu_5O_{16}. In other words, one of the multiple Cu effects is to suppress the hole redistribution effect. Therefore we understand that the spectrum shown in Fig. 7(a) is qualitatively the same as that in Fig. 2(a). If we take into account the O $2p$ band effects appropriately, single Cu site cluster models or a single-site Anderson impurity model can be a reasonable model in discussing the Cu $2p$ XPS.[17]

VI. SUMMARIES

In this study, we have examined the nonlocal screening effects pointed out by van Veenendaal and co-workers and proposed a HF-CI approximation for larger-cluster models.

Our calculations show that the two-line feature of the main structure given by van Veenendaal and co-workers is due primarily to their model where O $2p_\pi$ orbits were not taken into account. Convergence with respect to the cluster size was also insufficient. However, the convergence in the intensity ratio of the satellite to the main structure and the peak separation seem to be fairly good.

A merit of the HF-CI approximation proposed in the present study is apparently to reduce the Hamiltonian matrix size drastically. Since the matrix size increases exponentially with respect to the cluster size and the hole number, it is very difficult to treat large clusters by exact diagonalization calculations, such as $Cu_{25}O_{64}$. Consequently, we need some effective approximations. Our simple approximation clearly shows that we can derive an effective model from multiple Cu site models. This kind of approximation can be important in discussing early transition-metal compounds, such as VO_2 and $LaTiO_3$.

ACKNOWLEDGMENT

This work was partially supported by a Grant-in-Aid for Scientific Research from the Ministry of Education, Science and Culture, Japan.

*Electronic address: okada@ccyi.ccy.yamaguchi-u.ac.jp
†Electronic address: kotani@issp.u-tokyo.ac.jp

[1]M. A. van Veenendaal and G. A. Sawatzky, Phys. Rev. Lett. **70**, 2459 (1993).
[2]M. A. van Veenendaal, H. Eskes, and G. A. Sawatzky, Phys. Rev. B **47**, 11 462 (1993).
[3]M. A. van Veenendaal and G. A. Sawatzky, Phys. Rev. B **49**, 1407 (1994).
[4]M. A. van Veenendaal and G. A. Sawatzky, Phys. Rev. B **49**, 3473 (1994).
[5]A. Fujimori, E. Takayama-Muromachi, Y. Uchida, and B. Okai, Phys. Rev. B **35**, 8814 (1987).
[6]K. Okada and A. Kotani, J. Phys. Soc. Jpn. **58**, 1095 (1989).
[7]K. Okada and A. Kotani, J. Phys. Soc. Jpn. **58**, 2578 (1989).
[8]H. Eskes and G. A. Sawatzky, Phys. Rev. B **43**, 119 (1991).
[9]G. Chiaia, M. Qvarford, I. Lindau, S. Söderholm, U. O. Karlsson, S. A. Flodström, L. Leonyuk, A. Nilsson, and N. Mårtensson, Phys. Rev. B **51**, 1213 (1995).
[10]F. C. Zhang and T. M. Rice, Phys. Rev. B **37**, 3759 (1988).
[11]G. van der Laan, C. Westra, C. Haas, and G. A. Sawatzky, Phys. Rev. B **23**, 4369 (1981).
[12]V. Heine, in *Solid State Physics,* edited by H. Ehrenreich, F. Seitz, and D. Turnbull (Academic, New York, 1980), Vol. 35, p. 87.
[13]T. Nishino, J. Phys. Soc. Jpn. **59**, 4376 (1990).
[14]O. Gunnarsson and O. Jepsen, Phys. Rev. B **38**, 3568 (1988).
[15]K. Karlsson, O. Gunnarsson, and O. Jepsen, J. Phys. Condens. Matter **4**, 2801 (1992).
[16]W. A. Harisson, *Electronic Structure and the Properties of Solids* (Freeman, San Francisco, 1980).
[17]K. Okada, Y. Seino, and A. Kotani, J. Phys. Soc. Jpn. **60**, 1040 (1991).